Numerical simulations of interface cracks in layered magnetoelectroelastic solids under dynamic loadings

Michael Wünsche[1,*], Chuanzeng Zhang[1], Jan Sladek[2], Vladimir Sladek[2]

[1] Chair of Structural Mechanics, University of Siegen, D-57068 Siegen, Germany
[2] Institute of Construction and Architecture, Slovak Academy of Sciences, 84503 Bratislava, Slovakia
* Corresponding author: wuensche@bauwesen.uni-siegen.de

Abstract In this paper, transient dynamic crack analysis in two-dimensional, layered, anisotropic and linear magnetoelectroelastic solids is presented. For this purpose, a time-domain boundary element method (BEM) is developed. The layered magnetoelectroelastic solids are modeled by the multi-domain BEM formulation. The time-domain dynamic fundamental solutions for homogeneous and linear magnetoelectroelastic solids are applied in the present BEM. The spatial discretization of the boundary integral equations is performed by a Galerkin-method, while a collocation method is implemented for the temporal discretization of the arising convolution integrals. An explicit time-stepping scheme is obtained to compute the discrete boundary data including the generalized crack-opening-displacements (CODs). To show the effects of the interface, the material combinations and the dynamic loading on the intensity factors, numerical examples are presented and discussed.

Keywords transient dynamic crack analysis, linear magnetoelectroelastic solids, impact loading, interface-cracks, dynamic intensity factors.

1. Introduction

Magnetoelectroelastic materials offer many possibilities for advanced engineering structures due to their inherent coupling effects between mechanical, electrical and magnetic fields [3]. Important applications of magnetoelectroelastic materials are layered or laminated composites because they can be optimized to satisfy the high-performance requirements according to different in-service conditions. Beside cracks inside homogeneous domains, one of the most dominant failure mechanisms in layered or laminated composites is the interface failure. Interface cracks or interface debonding may be induced by the mismatch of the mechanical, electric, magnetic and thermal properties of the material constituents during the manufacturing process and the in-service loading conditions. Although the dynamic crack analysis in homogenous magnetoelectroelastic solids have been investigated by several authors (e.g., [5,6,7,9]) the corresponding investigation of interface cracks in layered magnetoelectroelastic solids is rather limited due to the problem complexity.
In this paper, an interface crack analysis in two-dimensional, layered and linear magnetoelectroelastic solids under impact loading is presented. For this purpose, a time-domain boundary element method (BEM) is developed. The layered magnetoelectroelastic solids are modeled by the multi-domain BEM formulation. The time-domain dynamic fundamental solutions for homogeneous and linear magnetoelectroelastic solids are applied in the present BEM. The spatial discretization of the boundary integral equations is performed by a Galerkin-method, while a collocation method is implemented for the temporal discretization of the arising convolution integrals. An explicit time-stepping scheme is obtained to compute the discrete boundary data including the generalized crack-opening-displacements (CODs). Since the asymptotic crack-tip field for an interface crack between two dissimilar anisotropic and linear magnetoelectroelastic materials shows different kinds of oscillating and non-oscillating singularities [1], which makes an implementation of a special crack-tip element somehow cumbersome, only standard elements are used at the crack-tips. For the accurate computation of the dynamic intensity factors the numerical error is minimized by a displacement-based extrapolation technique. To show the effects of the

interface, the material combinations and the dynamic loading on the intensity factors, numerical examples are presented and discussed.

2. Problem formulation

Let us consider a piecewise homogeneous, layered and linear magnetoelectroelastic solid with an interface crack as shown in Figure 1.

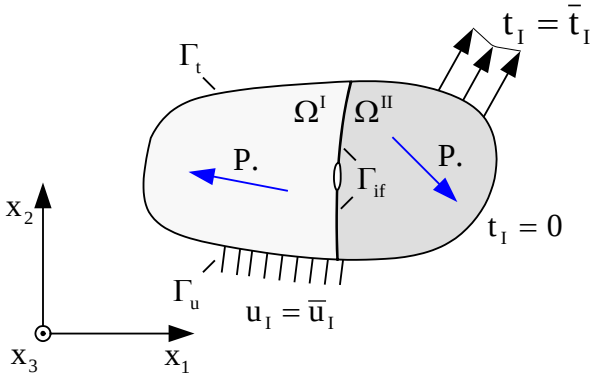

Figure 1. A cracked piecewise homogeneous and linear magnetoelectroelastic solid

In the absence of body forces, free electric charges, magnetic induction sources and applying the quasi-static assumption for the electric and magnetic fields, the cracked solid satisfies the generalized equations of motion

$$\sigma_{iJ,i}(\mathbf{x},t) = \rho^{\varsigma}\delta^{*}_{JK}\ddot{u}_K(\mathbf{x},t), \quad \delta^{*}_{JK} = \begin{cases} \delta_{JK}, J,K = 1,2 \\ 0, \text{otherwise} \end{cases}, \tag{1}$$

the constitutive equations

$$\sigma_{iJ}(\mathbf{x},t) = C^{\varsigma}_{iJKl}u_{K,l}(\mathbf{x},t), \tag{2}$$

where the generalized displacements, the generalized stresses and the generalized elasticity matrix C_{iJKl} for a homogenous domains Ω^{ζ} (ζ=1,2,…,N) are defined by

$$u_I = \begin{cases} u_i, I = 1,2 \\ \varphi, I = 4 \\ \phi, I = 5 \end{cases}, \quad \sigma_{iJ} = \begin{cases} \sigma_{iJ}, J = 1,2 \\ D_i, J = 4 \\ B_i, J = 5 \end{cases}, \quad C_{iJKl} = \begin{cases} c_{ijkl}, \ J,K = 1,2 \\ e_{lij}, \ J = 1,2, \quad K = 4 \\ h_{lij}, \ J = 1,2, \quad K = 5 \\ e_{ikl}, \ J = 4, \quad K = 1,2 \\ -\varepsilon_{il}, \ J,K = 4 \\ -\beta_{il}, \ J = 4, \quad K = 5 \\ h_{ikl}, \ J = 5, \quad K = 1,2 \\ -\beta_{il}, \ J = 5, \quad K = 4 \\ -\gamma_{il}, \ J,K = 5 \end{cases}, \tag{3}$$

the initial conditions

$$u_i(\mathbf{x}, t = 0) = \dot{u}_i(\mathbf{x}, t = 0) = 0, \tag{4}$$

the boundary conditions

$$t_I(\mathbf{x},t) = \bar{t}_I(\mathbf{x},t), \quad \mathbf{x} \in \Gamma_t, \tag{5}$$

$$u_I(\mathbf{x},t) = \bar{u}_I(\mathbf{x},t), \quad \mathbf{x} \in \Gamma_u, \tag{6}$$

and the continuity conditions on the interface without debonding

$$u_I^I(\mathbf{x},t) = u_I^{II}(\mathbf{x},t), \quad \mathbf{x} \in \Gamma_{if}, \tag{7}$$

$$t_I^I(\mathbf{x},t) = -t_I^{II}(\mathbf{x},t), \quad \mathbf{x} \in \Gamma_{if}. \tag{8}$$

In Eqs. (1)-(8), u_i, φ, Φ, σ_{ij}, D_i, B_i are the mechanical displacements, the electric potential, the magnetic potential, the mechanical stresses, the electric displacements and the magnetic inductions; ρ, c_{ijkl}, ε_{ij}, γ_{ij}, e_{ijk}, h_{ijk} and β_{ij} denote the mass density, the elasticity tensor, the dielectric permittivity tensor, the magnetic permittivity tensor, the piezoelectric tensor, the piezomagnetic tensor and the magnetoelectric tensor, respectively. Further, Γ_{if} is the interface between the homogenous domains Ω^{ζ} (ζ=1,2,…,N), Γ_t and Γ_u stand for the external boundaries where the generalized tractions t_I and the generalized displacements u_I are prescribed. The interface cracks are considered as free of mechanical stresses, electric displacements and magnetic inductions

$$\sigma_{iJ}(\mathbf{x} \in \Gamma_{c^+}, t) = \sigma_{iJ}(\mathbf{x} \in \Gamma_{c^-}, t) = 0, \tag{9}$$

where $\Gamma_{c\pm}$ are the two crack-faces. The generalized crack-opening-displacements (CODs) are defined by

$$\Delta u_I(\mathbf{x},t) = u_I(\mathbf{x} \in \Gamma_{c+}, t) - u_I(\mathbf{x} \in \Gamma_{c-}, t). \tag{10}$$

A comma after a quantity represents spatial derivatives while a dot over the quantity denotes time differentiation. Lower case Latin indices take the values 1 and 2 (elastic), while capital Latin indices take the values 1, 2 (elastic), 4 (electric) and 5 (magnetic).

3. Time-domain boundary integral equations

To solve the initial-boundary value problem, a spatial Galerkin-method is implemented, where the time-domain BIEs are treated in a weighted residual sense. The generalized time-domain displacement and traction BIEs can be written as

$$\int_\Gamma \psi(\mathbf{x})\, u_J(\mathbf{x},t)\, d\Gamma_x = \int_\Gamma \psi(\mathbf{x}) \int_\Gamma \left[u_{IJ}^G(\mathbf{x},\mathbf{y},t) * t_I(\mathbf{y},t) - t_{IJ}^G(\mathbf{x},\mathbf{y},t) * u_I(\mathbf{y},t) \right] d\Gamma_y d\Gamma_x, \tag{11}$$

$$\int_\Gamma \psi(\mathbf{x})\, t_J(\mathbf{x},t)\, d\Gamma_x = \int_\Gamma \psi(\mathbf{x}) \int_\Gamma \left[v_{IJ}^G(\mathbf{x},\mathbf{y},t) * t_I(\mathbf{y},t) - w_{IJ}^G(\mathbf{x},\mathbf{y},t) * u_I(\mathbf{y},t) \right] d\Gamma_y d\Gamma_x, \tag{12}$$

where ψ is the weighting function, an asterisk " * " denotes the Riemann convolution, $u_{IJ}^G(\mathbf{x},\mathbf{y},t)$, $t_{IJ}^G(\mathbf{x},\mathbf{y},t)$, $v_{IJ}^G(\mathbf{x},\mathbf{y},t)$ and $w_{IJ}^G(\mathbf{x},\mathbf{y},t)$ are the generalized displacement, traction and higher-order traction fundamental solutions. It should be mentioned that the dynamic time-domain fundamental solutions for homogeneous, anisotropic and linear magnetoelectroelastic solids are not available in an explicit form. In the two-dimensional case they can be expressed by a line integral over the unit-circle [4,9].

4. Numerical solution algorithm

A solution procedure is presented in this section to solve the time-domain BIEs (11) and (12) numerically. The procedure uses a Galerkin-method for the spatial discretization and a collocation method for the temporal discretization. A sub-domain technique is utilized, which divides the layered piecewise homogenous solid into two or several sub-domains with homogeneous material properties and to each sub-domain the time-domain BIEs (11) and (12) are applied. In the following, some details of the numerical solution algorithm are described. For the spatial discretization, the crack-faces, the external boundary of each homogeneous sub-domain and the interfaces are discretized by linear elements. Linear shape functions are also used for the temporal discretization in the present analysis. Since the asymptotic crack-tip field in the case of an interfacial crack between two dissimilar magnetoelectroelastic materials shows different oscillating and non-oscillating singularities in the generalized stress field, which makes an implementation of a special crack-tip element quite cumbersome, only standard elements are applied at the crack-tips. The strongly singular and hypersingular boundary integrals can be computed analytically by special

techniques. By using linear temporal shape-functions, time integrations can also be performed analytically. Only the line integrals over the unit-circle arising in the regular parts of the dynamic fundamental solutions have to be computed numerically by the standard Gaussian quadrature.
After temporal and spatial discretizations and considering the initial conditions the following systems of linear algebraic equations can be obtained for each sub-domain Ω^{ζ} (ζ=1,2,…,N)

$$\mathbf{C}_{\zeta}\,\mathbf{u}_{\zeta}^{\mathrm{K}} = \mathbf{U}_{\zeta}^{\mathrm{S}}\,\mathbf{t}_{\zeta}^{\mathrm{K}} - \mathbf{T}_{\zeta}^{\mathrm{S}}\,\mathbf{u}_{\zeta}^{\mathrm{K}} + \mathbf{T}_{\zeta}^{\mathrm{S}}\,\Delta\mathbf{u}_{\zeta}^{\mathrm{K}} + \sum_{\mathrm{k}=1}^{\mathrm{K}}\left[\mathbf{U}_{\zeta}^{\mathrm{D;K-k+1}}\,\mathbf{t}_{\zeta}^{\mathrm{k}} - \mathbf{T}_{\zeta}^{\mathrm{D;K-k+1}}\,\mathbf{u}_{\zeta}^{\mathrm{k}}\right], \tag{13}$$

$$\mathbf{D}_{\zeta}\,\mathbf{t}_{\zeta}^{\mathrm{K}} = \mathbf{V}_{\zeta}^{\mathrm{S}}\,\mathbf{t}_{\zeta}^{\mathrm{K}} - \mathbf{W}_{\zeta}^{\mathrm{S}}\,\mathbf{u}_{\zeta}^{\mathrm{K}} + \mathbf{W}_{\zeta}^{\mathrm{S}}\,\Delta\mathbf{u}_{\zeta}^{\mathrm{K}} + \sum_{\mathrm{k}=1}^{\mathrm{K}}\left[\mathbf{V}_{\zeta}^{\mathrm{D;K-k+1}}\,\mathbf{t}_{\zeta}^{\mathrm{k}} - \mathbf{W}_{\zeta}^{\mathrm{D;K-k+1}}\,\mathbf{u}_{\zeta}^{\mathrm{k}}\right]. \tag{14}$$

By invoking the continuity conditions (7) and (8) on the interface Γ_{if} and the crack-face boundary conditions (9) on Γ_{c^+} and Γ_{c^-}, and by considering the boundary conditions (5) and (6), Eqs. (13) and (14) can be summarized and recast into the following system of linear algebraic equations

$$\mathbf{x}^{\mathrm{K}} = (\mathbf{C}^{1})^{-1}\left[\mathbf{D}^{1}\,\mathbf{y}^{\mathrm{K}} + \sum_{\mathrm{k}=1}^{\mathrm{K-1}}(\mathbf{B}^{\mathrm{K-k+1}}\,\mathbf{t}^{\mathrm{k}} - \mathbf{A}^{\mathrm{K-k+1}}\,\mathbf{u}^{\mathrm{k}})\right], \tag{15}$$

where $\mathbf{y}^{\mathrm{K}}$ is the vector of the prescribed boundary data, $\mathbf{x}^{\mathrm{K}}$ represents the vector of the unknown boundary data, $\mathbf{A}^{\mathrm{k}}$, $\mathbf{B}^{\mathrm{k}}$, $\mathbf{C}^{1}$ and $\mathbf{D}^{1}$ are the system matrices. Eq. (15) can be computed time-step by time-step.

5. Intensity factors for an interfacial crack

The intensity factors for an interface crack between two dissimilar anisotropic and linear magnetoelectroelastic materials can be computed from the generalized crack-opening displacements (CODs)

$$\Delta\mathbf{u}(\mathrm{r}) = (\mathbf{H}+\overline{\mathbf{H}})\sqrt{\frac{\mathrm{r}}{2\pi}}\left[\frac{\mathrm{K}\mathrm{r}^{\mathrm{i}\varepsilon_1}\mathbf{w}}{(1+2\mathrm{i}\varepsilon_1)\cosh(\pi\varepsilon_1)} + \frac{\overline{\mathrm{K}}\mathrm{r}^{-\mathrm{i}\varepsilon_1}\overline{\mathbf{w}}}{(1-2\mathrm{i}\varepsilon_1)\cosh(\pi\varepsilon_1)} + \frac{\mathrm{K}_4\mathrm{r}^{-\varepsilon_2}\mathbf{w}_4}{(1-2\varepsilon_2)\cos(\pi\varepsilon_2)} + \mathrm{K}_5\mathbf{w}_5\right], \tag{16}$$

where $\mathrm{K}=\mathrm{K}_1+\mathrm{i}\mathrm{K}_2$, is the complex stress intensity factor, K_4 is the electric displacement intensity factor and K_5 is the magnetic induction intensity factor, ε_1 and ε_2 are the bimaterial constants, an overbar denotes the complex conjugate and i stands for the imaginary unit. The complex Hermitian matrix **H** is defined by

$$\mathbf{H} = \mathbf{Y}_{\mathrm{I}} + \overline{\mathbf{Y}}_{\mathrm{II}}, \quad \mathbf{Y}_{\mathrm{I}} = \mathrm{i}\mathbf{A}_{\mathrm{I}}\mathbf{B}_{\mathrm{I}}^{-1}, \quad \mathbf{Y}_{\mathrm{II}} = \mathrm{i}\mathbf{A}_{\mathrm{II}}\mathbf{B}_{\mathrm{II}}^{-1}, \tag{17}$$

where the subscripts I and II indicate the two layers. The matrices **A** and **B** are computed from the eigenvalue problem as shown in [1,2]. The two bimaterial constants ε_1 and ε_2 as well as the eigenvectors **w**, $\mathbf{w}_4$ and $\mathbf{w}_5$ are determined by the eigenvalue problem

$$\mathbf{D}^{-1}\mathbf{W}\mathbf{w} = -\mathrm{i}\beta\mathbf{w}, \tag{18}$$

with **D**=Re(**H**) and **W**=Im(**H**) being the real and the imaginary part of the matrix **H**. The eigenvalue β is either real or purely imaginary and related to the bimaterial constants by

$$\varepsilon_1 = \frac{1}{2}\ln\frac{1-\beta}{1+\beta}, \qquad \varepsilon_2 = \frac{1}{2}\ln\frac{1-\mathrm{i}\beta}{1+\mathrm{i}\beta}. \tag{19}$$

As shown by Eq. (16) the generalized crack-opening-displacements (CODs) in the crack-tip vicinity of interface cracks between two dissimilar linear magnetoelectroelastic materials show $\mathrm{a}\mathrm{r}^{1/2\pm\mathrm{i}\varepsilon}$-oscillating behavior and additionally a non-oscillating $\mathrm{r}^{1/2\pm\varepsilon}$-behavior. A similar behavior is known for interface cracks between two dissimilar piezoelectric materials [8]. This makes an implementation of special spatial crack-tip shape functions rather difficult. For this reason, only standard linear elements near the tips of interface cracks are used in this analysis. To minimize the numerical errors, a displacement-based extrapolation technique is applied to calculate the dynamic intensity factors from the numerically computed generalized crack-opening-displacements (CODs).

6. Numerical examples

In this section, numerical examples are presented and discussed to show the effects of the coupled fields, the interface, the material combinations and the dynamic loading on the dynamic intensity factors (IFs). The following loading parameters are introduced in order to measure the intensity of the electric and magnetic loading

$$\chi^{e}=\frac{e_{22}^{I}}{\varepsilon_{22}^{I}}\frac{D_0}{\sigma_0},\quad \chi^{m}=\frac{h_{22}^{I}}{\gamma_{22}^{I}}\frac{D_0}{\sigma_0}, \tag{20}$$

where σ_0, D_0 and B_0 are the mechanical, electric and magnetic loading amplitudes. For convenience of the presentation, the real part K_1 and the imaginary part K_2 of the complex dynamic stress intensity factors as well as the electric displacement intensity factor K_4 and the magnetic induction intensity factor K_5 of the interface crack are normalized by

$$K_1^{*}(t)=\frac{K_1(t)}{K_0},\quad K_2^{*}(t)=\frac{K_2(t)}{K_0},\quad K_4^{*}(t)=\frac{e_{22}^{I}}{\varepsilon_{22}^{I}}\frac{K_4(t)}{K_0},\quad K_5^{*}(t)=\frac{h_{22}^{I}}{\gamma_{22}^{I}}\frac{K_5(t)}{K_0}, \tag{21}$$

with $K_0=\sigma_0\sqrt{\pi a}$ and a is the half-length of an internal interface crack.

In the example we consider a central interface crack of length 2a in a rectangular, layered, anisotropic and linear magnetoelectroelastic plate with the poling direction normal to the interface crack as shown in Figure 2.

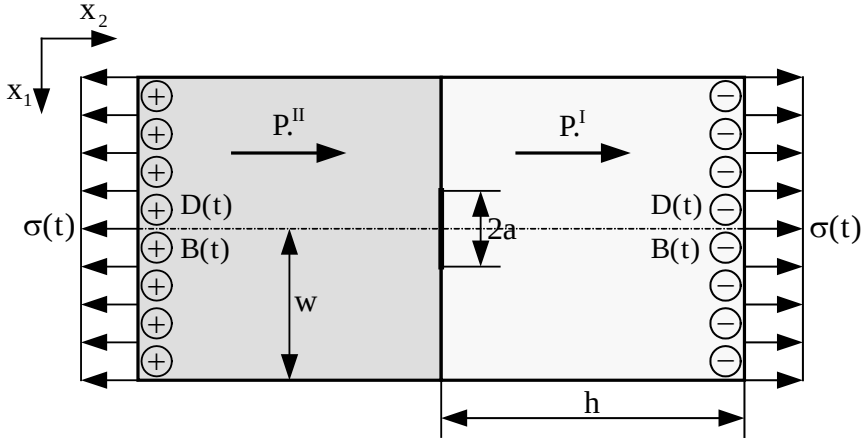

Figure 2. An interface crack in a rectangular layered magnetoelectroelastic plate

The cracked plate is subjected to an impact tensile loading $\sigma(t)=\sigma_0 H(t)$, an impact electric loading $D(t)=D_0 H(t)$ and an impact magnetic loading $B(t)=B_0 H(t)$, where H(t) denotes the Heaviside step function. The geometry is determined by h=20.0mm, w=10.0mm and 2a=4.8mm. The spatial discretization of the external boundary and the interface is performed by an element-length of 1.0mm. Each crack-face is approximated by 20 elements and a normalized time-step of $c_L\Delta t/h=0.05$ is chosen, where c_L is the quasi-longitudinal wave velocity. Numerical calculations are carried out for $BaTiO_3$-$CoFe_2O_4$ composite, with $BaTiO_3$ being its piezoelectric phase and $CoFe_2O_4$ its piezomagnetic phase. The magnetoelectroelastic material for the domain I has the constants

$$C_{11}=226.0\,\mathrm{GPa},\quad C_{12}=125.0\,\mathrm{GPa},\quad C_{22}=216.0\,\mathrm{GPa},\quad C_{66}=44.0\,\mathrm{GPa},$$
$$e_{16}=5.8\,\mathrm{C/m^2},\quad e_{21}=-2.2\,\mathrm{C/m^2},\quad e_{22}=9.3\,\mathrm{C/m^2},$$
$$h_{16}=275.0\,\mathrm{N/(Am)},\quad h_{21}=290.2\,\mathrm{N/(Am)},\quad h_{22}=350.0\,\mathrm{N/(Am)},$$
$$\varepsilon_{11}=56.4\,\mathrm{C^2/(GNm^2)},\quad \varepsilon_{22}=63.5\,\mathrm{C^2/(GNm^2)},$$
$$\beta_{11}=0.005367\,\mathrm{N/(GAV)},\quad \beta_{22}=2.7375\,\mathrm{N/(GAV)},$$
$$\gamma_{11}=297.0\,\mathrm{N/MA^2},\quad \gamma_{22}=83.5\,\mathrm{N/MA^2}, \tag{22}$$

while for domain II the material constants

$$C_{11} = 260.0\,GPa\,,\quad C_{12} = 150.0\,GPa\,,\quad C_{22} = 248.0\,GPa\,,\quad C_{66} = 45.0\,GPa\,,$$
$$e_{16} = 2.3\,C/m^2\,,\quad e_{21} = -0.9\,C/m^2\,,\quad e_{22} = 3.7\,C/m^2\,,$$
$$h_{16} = 440.0\,N/(Am)\,,\quad h_{21} = 464.2\,N/(Am)\,,\quad h_{22} = 560.0\,N/(Am)\,,$$
$$\varepsilon_{11} = 23.0\,C^2/(GNm^2)\,,\quad \varepsilon_{22} = 25.9\,C^2/(GNm^2)\,,$$
$$\beta_{11} = 0.0028\,N/(GAV)\,,\quad \beta_{22} = 2.0\,N/(GAV)\,,$$
$$\gamma_{11} = 473.0\,N/MA^2\,,\quad \gamma_{22} = 127.6\,N/MA^2\,, \tag{23}$$

are applied. The numerical results of the present time-domain BEM obtained for different loading combinations and the application of material (22) for both layers are presented in Figure 3. This special case is equal to an interior crack inside a homogenous magnetoelectroelastic plate and the intensity factors are given in [9]. The normalized dynamic intensity factors for the interface crack are shown in Figure 4.

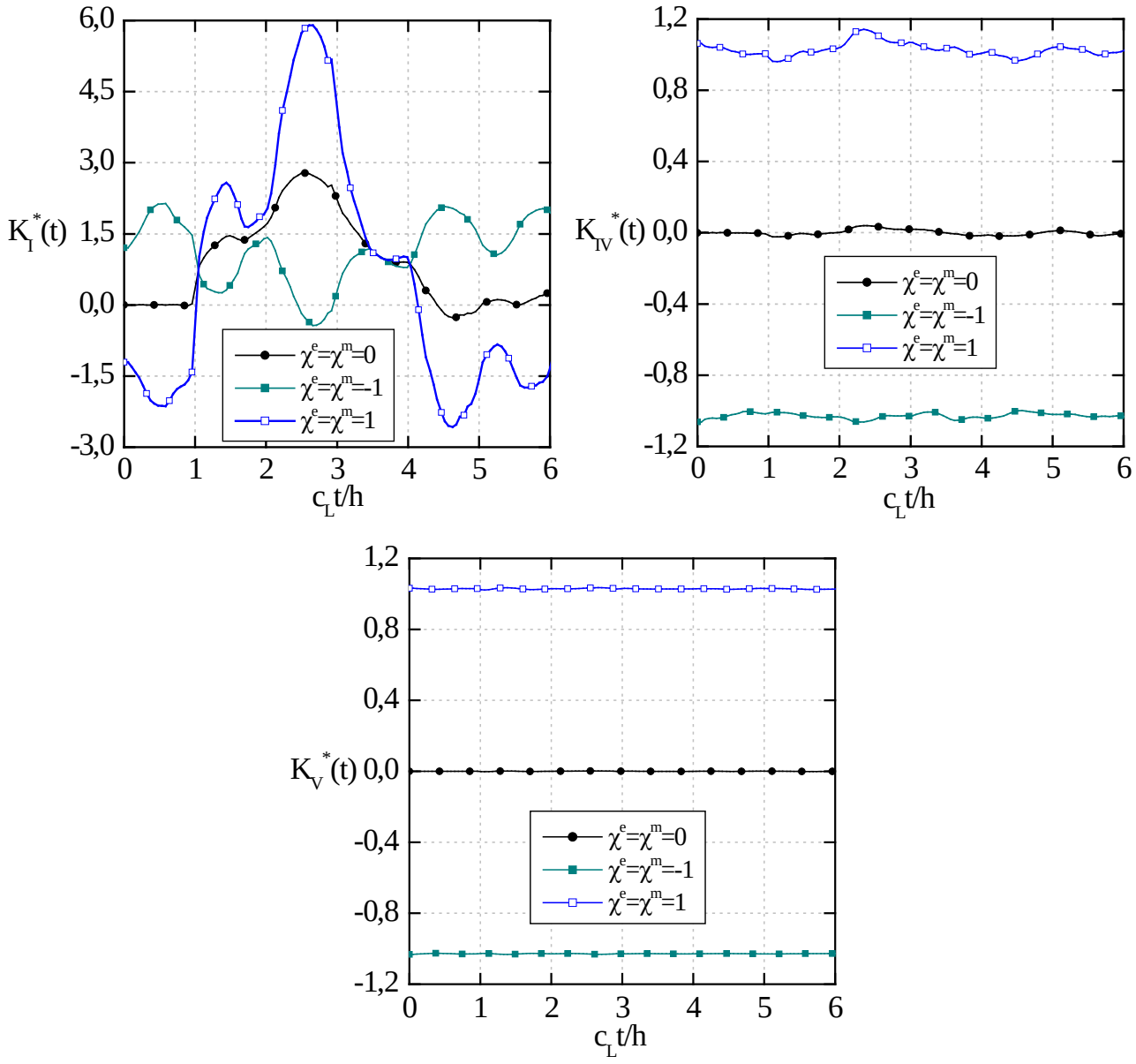

Figure 3. Normalized dynamic intensity factors for an interior crack subjected to different loadings

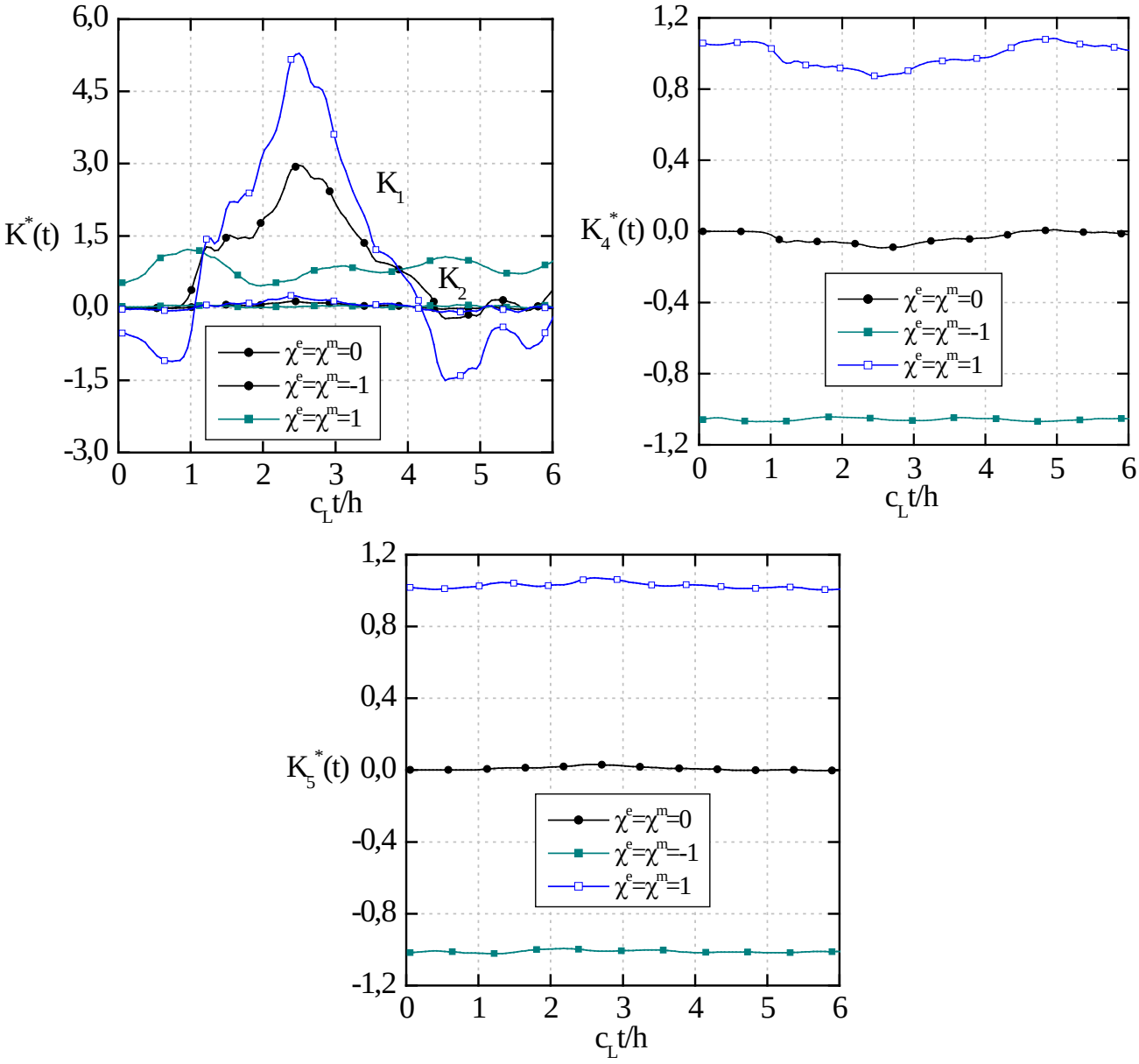

Figure 4. Normalized dynamic intensity factors for an interface crack subjected to different loadings

The normalized dynamic mode-I, mode-IV and mode-V intensity factors for an interior crack in a homogenous magnetoelectroelastic plate as well as the real part of the complex intensity factor, the electrical displacement intensity factor and the magnetic induction intensity factor for the interface crack obtained by the present TDBEM have a similar global behavior. The mode-II intensity factors vanish, since no shear stress components are induced for all applied loadings in the case of a transversely isotropic material behavior. In contrast, the crack opening and sliding modes I and II are coupled each other for the interface crack and therefore the imaginary part of the complex intensity factor is unequal zero. It can be observed that, when an electric and magnetic impact is applied, the normalized dynamic mode-I stress intensity factor and the complex stress intensity factor start from a non-zero value at t=0. This is due to the quasi-static assumption on the electromagnetic fields, which implies that the cracked magnetoelectroelatic plate is immediately subjected to an electromagnetic wave and therefore the crack opens at t=0. In contrast, the elastic waves induced by the mechanical impact need some time to reach and excite the crack, as clearly observed for the case $\chi^e=\chi^m=0$. It should further be mentioned here, that the applied electric and

magnetic loading may lead to a physically meaningless crack-face intersection in different time ranges for the case $\chi^e=\chi^m=1$. This requires an advanced iterative solution procedure for the crack-face contact analysis which is not considered in this work. The peak values of the normalized dynamic intensity factors decrease with increasing electric and magnetic loading amplitudes.

Acknowledgements

This work is supported by the German Research Foundation (DFG) under the project number ZH 15/14-1 and by the Slovak Science and Technology Assistance Agency registered under the number APVV-0014-10. The financial support is gratefully acknowledged.

References

[1] C.-F. Gao, P. Tong, T.-Y. Zhang, Interfacial crack problems in magneto-electroelastic solids. International Journal of Engineering Science, 41 (2003) 2105-2121.
[2] C. Fan, Y. Zhou, H. Wang, M. Zhao, Singular behaviors of interfacial cracks in 2D magnetoelectroelastic bimaterials. Acta Mechanica Solida Sinica, 22 (2009) 232-239.
[3] C.W. Nan, Magnetoelectric effect in composite of piezoelectric and piezomagnetic phases. Phys. Rev. B, 50 (1994) 6082-6088.
[4] R. Rojas-Díaz, A. Sáez, F. García-Sánchez, Ch. Zhang, Time-harmonic Green's functions for anisotropic magnetoelectroelasticity. International Journal of Solids and Structures, 45 (2008) 144-158.
[5] R. Rojas-Díaz, F. García-Sánchez, A. Sáez, E. Rodríguez-Mayorga, Ch. Zhang, Fracture analysis of plane piezoelectric/piezomagnetic multiphase composites under transient loading. Computer Methods in Applied Mechanics and Engineering, 200 (2011) 2931-2942.
[6] J. Sladek, V. Sladek, P. Solek, E. Pan, Fracture analysis of cracks in magneto-electro-elastic solids by the MLPG. Computational Mechanics, 42 (2008) 697-714.
[7] J. Sladek, V. Sladek, P. Stanak, Ch. Zhang, M. Wünsche, An interaction integral method for computing fracture parameters in functionally graded magnetoelectroelastic composites. Computer, Materials and Continua, 23 (2011) 35-68.
[8] Z. Suo, C.M. Kuo, D.M. Barnett, J.R. Willis, Fracture mechanics for piezoelectric ceramics. Journal of the Mechanics and Physics of Solids, 40 (1992) 739-765.
[9] M. Wünsche, A. Sáez, F. García-Sánchez, Ch. Zhang, Transient dynamic analysis of cracked magnetoelectroelastic solids by a time-domain BEM. European Journal of Mechanics - A/Solids, 32 (2012) 118-130.